Figure 2, the difference in the SCF and MBPT(2) spectra of triimide is exaggerated due to the large anomalous SCF intensity of 839 km/mol. However, changes in relative peak heights may still be observed.

The two spectra of triazene in Figure 3 perhaps provide the best correspondence between the two levels of theory. At the MBPT(2) level the frequencies of the band centers are lower and the relative intensities of the stronger bands between 1000 and 2000 wavenumbers have leveled out to approximately the same peak height. Other than this, there appears to be little difference. However, recall that the order of two of the bands has shifted in the MBPT(2) results from the SCF order.

The SCF-DZP spectra for the two cis isomers are presented in Figure 4. The D_{3h} symmetry of *cis*-triaziridine causes many of the frequencies of its normal modes to be degenerate. This degeneracy is easily observed in the spectrum by the relatively few distinct band centers. As with triimide, the accuracy of the SCF spectrum for *cis*-triimide is diminished by the large anomalous intensities.

V. Conclusions

The optimum structures of triazene, triimide, and triaziridine have been determined for the 6-31G* basis set and the DZP basis set at the SCF level and for the DZP basis set at the MBPT(2) level of electron correlation. Relative electronic energies have been obtained with SDTQ-MBPT(4) and CCSD augmented by T(CCSD). The structures we have found agree with previously reported results, except that our results using polarized basis sets indicate that the structure of triazene is not exactly planar. Vibrational analyses of these structures have been carried out at all three levels of theory. We have predicted infrared spectra of the important isomers with electron correlation. The vibrational frequencies and moments of inertia have been used to compute thermochemical properties of the molecules, including the free energy.

Experimental and theoretical evidence suggests that some of these molecules can be isolated at room temperature. Low-temperature isolation of these compounds would very likely succeed. The predicted infrared spectra and thermochemical properties should aid experimental attempts to synthesize and isolate these compounds.

We feel we now have a good understanding of the relative thermodynamic stabilities of the N_3H_3 molecules, but we must do more work to understand the kinetic lability of these compounds. By using a 6-31G* basis set, we have found one SCF transition state between triaziridine and triimide. The energy barrier that this transition state represents is large enough for triaziridine to be fairly stable, but further work needs to be done with a larger basis set. In addition, this transition state deserves further attention because it appears to violate the Hammond postulate. Other transition states also need to be found to assess the kinetic stability of the various N_3H_3 isomers. Nguyen et al. claim to have found a variety of transition states on the N_3H_3 surface, but their description of the search routine leads us to believe their transition structures are not necessarily points of zero force on the surface. Interestingly, the transition state we report here is not one found by Nguyen et al. In future work we plan to make a systematic search for transition states by using large basis sets and correlation. Another goal is the computation of electronic spectra for the principal isomers using the newly developed equation-of-motion coupled-cluster excitation energy scheme.[52]

Acknowledgment. We thank Professor Willis Person for many helpful discussions on infrared spectra. R.J.B. acknowledges support of the U.S. Air Force Office of Scientific Research (Grant AFOSR-85-0011) and the U.S. Army Research Office (Contract No. DAAG29-84-K-0025). B.A.H. and L.J.S. thank the National Science Foundation (Grant No. CHE 8605951) for support of part of this work, and C.S. is grateful for partial support by the Air Force Office of Scientific Research (Grant AFOSR-83-0110).

Registry No. 1, 6572-31-2; *cis*-1, 108739-42-0; 6, 15056-34-5; *cis*-6, 58729-78-5.

(52) Rittby, M.; Magers, D. H.; Brown, R. E.; Bartlett, R. J., to be published.

A Protocol for Determining Enantioselective Binding of Chiral Analytes on Chiral Chromatographic Surfaces

Kenny B. Lipkowitz,*† David A. Demeter,† Richard Zegarra,† Raima Larter,† and Thomas Darden‡

Contribution from the Department of Chemistry, Indiana-Purdue University, Indianapolis, Indiana 46223, and the Laboratory of Molecular Biophysics, National Institute of Environmental Health Science, PO Box 12233, Research Triangle Park, North Carolina 27709.
Received October 26, 1987

Abstract: A protocol for estimating binding energies of optical isomers to chiral surfaces used in chromatography is developed. The conformational states of the analyte and of the chiral stationary phase are explicitly treated. Enantioselective binding of (*S*)-(+)-2,2,2-trifluoro-1-(9-anthryl)ethanol to a chiral surface is found to be conformation dependent. Regions around the chiral stationary phase responsible for the enantiodifferentiation are located and a new chiral recognition model is presented as an alternative to a previously published model.

I. Introduction

Methods have been developed to separate optical isomers by direct resolution of enantiomeric mixtures. The most promising of these techniques utilize chromatographic separation with chiral stationary phases (CSP). While the search for suitable chiral phases has been challenging, some success has been achieved for gas, liquid, and planar chromatographies. These developments are summarized in several review articles,[1] proceedings of a

† Indiana-Purdue University.
‡ National Institute of Environmental Health Science.

(1) Leading references of reviews can be found in the following: Armstrong, D. W. *Anal. Chem.* **1987**, *59*(2), 84A.

0002-7863/88/1510-3446$01.50/0

conference,[2] and a book dedicated to the chromatographic separation of stereoisomers.[3]

The way in which these chromatographic surfaces separate enantiomers is not known. Therefore, we initiated a research project designed to uncover the molecular interactions responsible for enantioselective binding. Although our interests are directed toward chiral separation in chromatography, our results have immediate application to other areas of science where chiral discrimination is important such as in drug design. Our current goals are to predict which of two optical analytes is longer retained on a chiral column and to assess the structural features of the transient diastereomeric complexes that are responsible for analyte stereodifferentiation. This in turn empowers us with the ability to formulate chiral recognition models and ultimately to design improved versions of existing chiral stationary phases.

We take a theoretical approach, using molecular orbital theory, molecular mechanics, statistical thermodynamics, and molecular graphics, to solve the problem. We are not the first group to study the discriminating interactions between chiral molecules with theory.[4-8] Unfortunately most other groups employ highly stylized models that are not amenable to molecules of interest to most chemists.[9] Our approach is general and uses software available to most laboratories.[10]

In the next section of this paper we provide a theoretical foundation for the work. In Section III we describe new algorithms developed and introduce the chromatographic system to be modeled. In Section IV we present the results of our analysis, and in Section V we interpret these results in light of existing chiral recognition models.

II. Theory

Consider the following equilibria which occur throughout a chromatographic column:

$$C^R + A^R \rightleftharpoons C^R{\cdot}A^R \quad (1)$$

$$C^R + A^S \rightleftharpoons C^R{\cdot}A^S \quad (2)$$

C is the chiral stationary phase, A the analyte, and the superscripts R and S the Cahn–Prelog–Ingold stereochemical assignments. Each equilibrium is associated with a free energy of binding, ΔG. These free energies contain the information needed to predict the elution order of chiral analytes; the analyte which is more tightly bound to the CSP has a more negative ΔG and will be most retained.

One need not, however, assess ΔG for each equilibrium. Rather, we need only to compute G for the $C^R{\cdot}A^R$ complex and compare it directly with G of the $C^R{\cdot}A^S$ complex. This direct comparison is possible because the left-hand sides of both equilibria are chemically identical. In other words, the free energy of the R form of the unbound analyte is the same as the free energy of the S form. This is ensured by their enantiomeric relationship.

The Gibbs free energy of a specific complex is a macroscopic thermodynamic quantity that represents a weighted average of all possible microscopic diastereomeric complexes. The enthalpic component of the free energy is defined as

$$H = U + PV \quad (3)$$

where U is the internal energy of the system and PV is the work function. In our system, $\Delta(PV) = 0$ since no expansion or contraction occurs; hence $\Delta H = \Delta U$. The entropic part of the free energy is obtained from:[11]

$$S = -k \sum_i p_i \ln p_i \quad (4)$$

where k is the Boltzmann constant and p_i is the probability of microstate i. For our purposes, a microstate is any unique orientation of the CSP and analyte in a diastereomeric complex. The value of H for the diastereomeric complexes in (1) and (2) can be obtained from molecular mechanics calculations. The probabilities, p_i, of each of the microstates are then calculated by determining the Boltzmann distribution of all the enthalpies.

Two important assumptions invoked in our approach concern the roles of the stationary phase and the solvent. Because the nature of organic supports on a silica surface is not well understood, we assume a 1:1 ratio of CSP:analyte. Lightly loaded columns may in fact have an inhomogeneous distribution of the CSP on the silica support. There may exist high-density regions of CSP into which the analyte may dissolve, but here we assume that one CSP molecule interacts with one analyte molecule.[12] Furthermore, we will assume that the silica support to which the CSP is attached has no influence on the chiral discrimination so will not be considered. Second, the solvent is not explicitly included in the model. We recognize that optical isomers are equivalently solvated as they flow in the bulk solvent, and upon complexation with the chiral surface, they need to partially desolvate or undergo a major solvent reorganization to form a complex. The complexes which form, being diastereomers, will not be equivalently solvated. Furthermore intramolecular hydrogen bonds between analyte and CSP are expected to be weakened by hydrogen bonding solvents, and even non-hydrogen bonding solvents may have a profound effect upon the stabilization of these complexes. In due course we will evaluate the differential stabilization of these diastereomeric complexes by explicitly incorporating solvent molecules. Nonetheless, we have evidence that this is an effect which, to a first approximation, may be neglected.[13]

With these assumptions, we are able to calculate an approximate free energy of interaction for the system. We will refer to this free energy as a column-averaged interaction energy, $\bar{E}$. The energy of each diastereomeric complex depends on the shape of the CSP, the shape of the analyte (A), and the orientation of the

(2) *J. Liq. Chromatogr.* **1986**, 9. Hara, S.; Cazes, J., Eds. *J. Liq. Chromatogr.* **1986**, *9*(2–3), 243.

(3) Souter, R. W. *Chromatographic Separations of Stereoisomers*; CRC Press: Boca Raton, 1985.

(4) (a) Craig, D. P.; Power, E. A.; Thirunamachandran, T. *Proc. R. Soc. London* **1971**, *A322*, 165. (b) Craig, D. P.; Schipper, P. E. *Proc. R. Soc. London* **1975**, *A342*, 19. (c) Craig, D. P.; Radom, L.; Stiles, P. J. *Proc. R. Soc. London* **1975**, *A343*, 11. (d) Craig, D. P.; Mellor, D. P. *Top. Curr. Chem.* **1976**, *63*, 1. (e) Craig, D. P. In *Optical Activity and Chiral Discimination*; Mason, S. F., Ed.; Reidel: Dordrecht, 1979.

(5) (a) Schipper, P. E. *Chem. Phys.* **1977**, *26*, 29. (b) Schipper, P. E. *Chem. Phys.* **1979**, *44*, 261. (c) Schipper, P. E. *Aust. J. Chem.* **1982**, *35*, 1513.

(6) (a) Girardt, C.; Vega, L. *Surf. Sci.* **1985**, *151*, 447. (b) Vega, L.; Breton, J.; Girardt, C.; Galatry, L. *J. Chem. Phys.* **1986**, *84*(*9*), 5171. (c) Kerdye, A.; Galatry, L. *Mol. Phys.* **1985**, *55*(*6*), 1383.

(7) (a) Huckaby, D. A.; Ausloos, M.; Clippe, P. *J. Chem. Phys.* **1985**, *82*(*11*), 5040. (b) Huckaby, D. A.; Shinmi, M.; Ausloos, M.; Clippe, P. *J. Chem. Phys.* **1986**, *84*(*9*), 5090.

(8) Salem, L.; Chapuisat, X.; Segal, G.; Hiberty, P. C.; Minot, C.; Leforestier, C.; Sautet, P. *J. Am. Chem. Soc.* **1987**, *109*, 2887.

(9) An exception is the molecular modeling study of (+) and (−) warfarin binding to β-cyclodextrin: Armstrong, D. W.; Ward, T. J.; Armstong, R. D.; Beesley, T. E. *Science* **1986**, *232*, 1132.

(10) Most of the programs we use are available from the Quantum Chemistry Program Exchange, Department of Chemistry, Indiana University, Bloomington, IN 47405. All modeling programs and new algorithms developed here are available from the authors.

(11) McQuarrie, D. A. *Statistical Mechanics*; Harper and Row: New York, 1976.

(12) There is evidence supporting this: Däppen, R.; Meyer, V. R.; Arm, H. *J. Chromatogr.* **1986**, *361*, 93.

(13) Trifluoroanthrylethanols have been separated on an (*R*)-phenylglycine CSP with a mobile phase of 95% hexane and 5% 2-propanol. The propanol is the solvent component most likely to be involved in the complexation due to its ability to hydrogen bond with both the analyte and the CSP. Studies done on the effect of this mobile phase modifier show that decreasing the amount of 2-propanol increases the separation factor, α. Pirkle, W. H.; House, D. W.; Finn, J. M. *J. Chromatogr.* **1980**, *192*, 143. This implies that 2-propanol does not contribute to the mechanism of chiral recognition and validates our assumption of neglecting the explicit presence of solvent molecules.

(14) A major concern of ours is how best to treat the shape of these organic phases. Our initial approach was to use the most stable conformation of the CSP and of the analyte. In some instances this is valid but in others, especially for flexible CSP's whose conformational potential energy surface has multiple minima and/or is flat, this is improper. It is possible that a thermally accessible, high-energy conformer of the CSP is responsible for the separation. Similar concerns are expressed in the pharmaceutical industry where the "active conformation" of a drug does not correspond to its global minimum on the potential energy surface.

two relative to one another. The column average interaction energy, $\bar{E}$, then, takes into account the probability that the CSP is in a particular conformation, the probability that A is in a particular conformation, as well as the probability that the two are oriented in a particular way in the complex.

The first two probabilities are relatively straightforward to determine if one assumes that the relaxation of the CSP into a specific conformational state occurs independently of A, and the relaxation of A occurs independently of the CSP. In other words, to determine the individual conformations, both the CSP and the analyte can be treated as isolated molecules. Once the conformations exist, we assume a complex forms between the two rigid bodies. Suppose that such an analysis of the CSP yields a potential energy surface with a large number of minima. If there are l minima, the probability that the CSP will be in the hth minimum is given by a Boltzmann distribution

$$P_h = \frac{\exp(-E_{\mathrm{CSP},h}/kT)}{\sum_{h'=1}^{l} \exp(-E_{\mathrm{CSP},h'}/kT)} \tag{5}$$

where $E_{\mathrm{CSP},h}$ is the energy of the hth minimum and P_h is the desired probability. A similar analysis of the analyte conformations will yield a surface with some number, m, of minima. The probability that the analyte will be in the ith minimum is given by

$$Q_i = \frac{\exp(-E_{\mathrm{A},i}/kT)}{\sum_{i'=1}^{m} \exp(-E_{\mathrm{A},i'}/kT)} \tag{6}$$

where $E_{\mathrm{A},i}$ is the energy of the ith conformational state of A.

If there are l possible conformations of the CSP and m possible conformations of A, we must consider lm combinations of A docking with the CSP. Furthermore, for each of these combinations we consider all conceivable orientations between the CSP and A since each unique orientation corresponds to a unique energy state for that combination of conformers in the complex. Hence, the probability that the complex forms between the CSP in the hth conformation and A in the ith conformation with the jth intermolecular orientation of energy ϵ_{hij} is given by

$$R_{hij} = \frac{\exp(-\epsilon_{hij}/kT)}{\sum_{j'=1}^{n} \exp(-\epsilon_{hij'}/kT)} \tag{7}$$

In our equations, we represent the microscopic enthalpy of the complex as ϵ_{hij}.

P_h, Q_i, and R_{hij} are the three weighting factors used in the rigid body model for estimating the Gibbs free energy of the complex. The enthalpies of the complexes, ϵ_{hij}, are obtained from molecular mechanics calculations. The entropic term for each unique diastereomeric complex is calculated from the corresponding enthalpy as follows.

A Boltzmann distribution is obtained for all the calculated enthalpies due to the lm combinations of A docking with CSP. The probability of each unique diastereomeric complex, p_{hij}, is expressed as

$$p_{hij} = \frac{\exp(-\epsilon_{hij}/kT)}{\sum_{h'=1}^{l}\sum_{i'=1}^{m}\sum_{j'=1}^{n} \exp(-\epsilon_{h'i'j'}/kT)} \tag{8}$$

The entropy at temperature T is then calculated from the probabilities

$$Ts_{hij} = -kTp_{hij} \ln p_{hij} \tag{9}$$

Combining ϵ_{hij} and Ts_{hij}, the Gibbs free energy of each unique diastereomeric complex, g_{hij}, is calculated

$$g_{hij} = \epsilon_{hij} - Ts_{hij} \tag{10}$$

The average interaction energy of each type of complex is, thus,

$$\bar{g}_{hi} = \sum_{j=1}^{n} R_{hij} g_{hij} \tag{11}$$

where the sum runs over the different orientations of the complex between the CSP in the hth conformation and the analyte in the ith conformation. To determine the average interaction energy between the CSP and A in the column as a whole, we must take into account the distribution over the conformational states of each partner in the complex. The column average interaction energy is, thus,

$$\bar{E} = \sum_{h=1}^{l}\sum_{i=1}^{m} P_h Q_i \bar{g}_{hi} \tag{12}$$

Substituting the definitions of P_h, Q_i, and $\bar{g}_{hi}$ we find the explicit expression for the column average interaction energy:

$$\bar{E} = \sum_{h=1}^{l}\sum_{i=1}^{m}\left(\frac{\exp(-E_{\mathrm{CSP},h}/kT)}{\sum_{h'=1}^{l} \exp(-E_{\mathrm{CSP},h'}/kT)}\right)\left(\frac{\exp(-E_{\mathrm{A},i}/kT)}{\sum_{i'=1}^{m} \exp(-E_{\mathrm{A},i'}/kT)}\right) \sum_{j=1}^{n} g_{hij}\left(\frac{\exp(-\epsilon_{hij}/kT)}{\sum_{j'=1}^{n} \exp(-\epsilon_{hij'}/kT)}\right) \tag{13}$$

Equation 13 represents our approximation of the macroscopic free energy of interaction and includes factors representing average conformations of the CSP and of the analyte as well as the average orientations of the complexes.

III. Model

A. Computational Methods. All model building and structure manipulation were performed with MODEL, an interactive graphics program originally constructed by W. Clark Still of Columbia University and extended by us for the work described here. The program is available from the authors and an enhanced version will be submitted to the Quantum Chemistry Program Exchange.

Molecular orbital calculations were carried out with Stewart's MOPAC program.[15] The MNDO hamiltonian was employed throughout. Structures were assumed to be ground-state singlets and all internal degrees of freedom were fully optimized unless stated otherwise. The empirical force field employed was MM2 with the original parameter set.[16] A thorough overview of SCF molecular orbital and empirical force field methods has recently been published[17] so the merits of each will not be discussed here. In some instances structures were computed with both the MM2D and MM2C methods. MM2D refers to the MM2 force field with bond dipoles and MM2C refers to the MM2 force field with point charges derived from MNDO calculations.

The systematic sampling of the possible diastereromeric complexes is done using rigid components. Both CSP and analyte are held fixed in a minimum energy conformation found during their respective conformational analysis.

The position of the analyte with respect to the CSP is chosen in the following way. The chiral center of each molecule is defined as an origin for that molecule. The position of the origin of the analyte with respect to the origin of the CSP is defined by a set of spherical polar coordinates, r θ, ϕ (see Figure 1). For a fixed value of r, the origin of the analyte will, thus, lie somewhere on the surface of a sphere of radius r around the CSP and the position on the sphere will be defined by the two angles θ and ϕ.

The atoms which make up the analyte and CSP are at positions that are defined in terms of local, molecular coordinate systems.

(15) Throughout this study we used the MNDO hamiltonian (Dewar, M. J. S.; Thiel, W. *J. Am. Chem. Soc.* **1977**, *99*, 4899) as implemented in MOPAC Stewart, J. P. *QCPE Bulletin* **1983**, *3*(2), 455).

(16) The MM2 force field: Allinger, N. L.; Yuh, Y. H. *QCPE* **1981**, *13*, 395.

(17) Clark, T. *A Handbook* of Computational *Chemistry*: *A Practical Guide to Chemical Structure and Energy Calculations*; Wiley-Interscience: New York, 1985.

These coordinates would normally be Cartesian coordinates defined relative to the origin at the chiral center. The orientation of the set of axes on the analyte with respect to the set on the CSP must also be defined, then, to specify the positions of the atoms in the analyte with respect to those in the CSP. A pair of Euler angles[18] are defined, then, which give the relative orientation of the analyte molecular axes and the CSP molecular axes.

The distance r between the origins of the CSP and analyte is chosen in such a way that the molecules are just "touching". The distance r, then, depends on the positions of the atoms in both molecules and their van der Waals radii. For fixed values of θ and ϕ and fixed Euler angles, the square of the distance between an atom in the CSP and an atom in the analyte is a quadratic function of r. Taking the atom–atom distance to be the distance at which van der Waals spheres of the atoms just touch, the quadratic equation can be solved for r. The largest root of these quadratic equations is the distance at which the molecules just touch.

The computational procedure, then, is to choose a value of r at which the molecules just touch and values of θ and ϕ to define the position of the analyte with respect to the CSP. The intermolecular energy is computed for a whole set of Euler angles, also chosen in a uniform way. A new pair of values of θ and ϕ are chosen and the procedure repeated until all angles on the sphere have been uniformly sampled.

Saving the lowest energy configuration (i.e., pair of Euler angles for which the intermolecular energy is lowest) for each value of r, θ, and ϕ allows us to create a plot which represents the intermolecular energy between the two rigid molecules as we tumble the analyte over the van der Waals surface of the CSP. It is important to note that both analytes are treated the same way; the origins are identical, the axes are the same, and the manner in which analyte is tumbled over the CSP is precisely the same for both optical isomers.

B. System Studied. We focus our attention on the resolution of (±)-2,2,2-trifluoro-1-(9-anthryl)ethanol (**1**) on 3,5-dinitrobenzoyl-phenylglycine CSP (**2**). We select this phase because (i) it is commercially available and is already well established in many

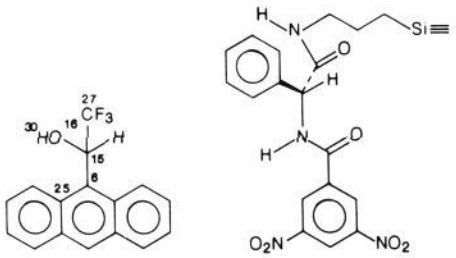

1 2

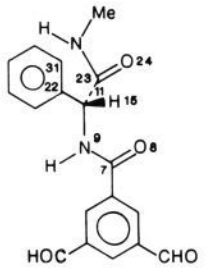

3

laboratories,[19] (ii) it is possible to make simple structural modifications for future QSAR studies, (iii) its chromatographic properties have been thoroughly explored,[20,21] (iv) a chiral recognition model has been proposed,[21a] and (v) it is an interesting CSP because it can adopt a multitude of shapes. The analyte was selected because it is used as a chiral shift additive in NMR spectroscopy[22] and serves as the standard for quality-control tests of commercially available columns.[23]

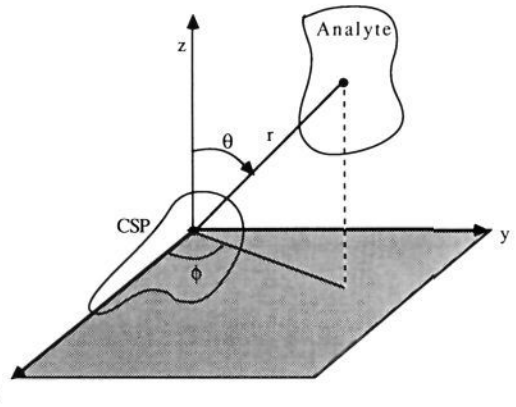

Figure 1. Position of analyte with respect to the chiral stationary phase represented by spherical coordinates (r, θ, ϕ).

Table I. Fully Relaxed MM2D Geometries of *R*-CSP Analogue **3**

name	Torsion Angles (deg) ω C_7–N_9–C_{11}–H_{15}	δ N_9–C_{11}–C_{23}–O_{24}	ρ H_{15}–C_{11}–C_{22}–C_{31}	rel energy (kcal mol^{-1})
CSP1	−60.1	−132.0	19.1	0.00
CSP2	−165.2	140.2	155.4	1.46
CSP3	41.2	118.7	19.2	2.75
CSP4	−62.0	17.1	162.4	3.55
CSP5	−30.5	109.3	43.4	4.31

Rather than doing calculations on the entire CSP which is attached by a spacer chain to silica, we use CSP analogue **3**. Note that the propyl chain has been replaced with a methyl group. On the one hand this simplifies the computation but on the other it neglects the interactions of analyte with the spacer chain and the silica surface. Also note that the NO_2 groups in **2** have been replaced by CHO groups in **3**. This is required because MM2 parameters for nitro groups do not yet exist. The purpose of the NO_2 groups in **2** is to induce formation of a charge-transfer complex between the CSP and analytes bearing aryl groups. MM2 accounts for this type of interaction because of its propensity to overestimate π-face attractions between aromatic chromophores.[24] Finally the amide bonds were assumed to be planar and in the Z configuration.[25]

IV. Results

A. Conformational Analysis. To determine P_h in eq 5 it is necessary to perform an analysis of the conformational states accessible to the CSP. The conformations accessible to **3** along with related phases (both covalent and ionic) have been addressed by us[26] and others[27] employing MM2C and MM2D force fields

(18) Goldstein, H. *Classical Mechanics*; Addison-Wesley Publishing Co.: Reading, MA 1950.
(19) Available from: Alltech Associates, 2051 Waukegan Rd., Deerfield, IL, 60015; Baker, J. T., 222 Red School Lane, Phillipsburg, NJ, 00865; Regis, 8210 Austin Ave., Morton Grove, IL 60053.
(20) Wainer, I. W.; Doyle, T. D. *LC Magazine* **1984**, *2*, 88.
(21) (a) Pirkle, W. H.; House, D. W.; Finn, J. M. *J. Chromatogr.* **1980**, *192*, 143–158. (b) Pirkle, W. H.; Finn, J. M.; Schreiner, J. L.; Hampton, B. C. *J. Am. Chem. Soc.* **1981**, *103*, 3964. (c) Pirkle, W. H.; Finn, J. M. *J. Org. Chem.* **1981**, *46*, 2935. (d) Pirkle, W. H.; Schreiner, J. L. *Ibid.* **1981**, *46*, 4988. (e) Pirkle, W. H.; Finn, J. M. *Ibid.* **1982**, *47*, 4037. (f) Pirkle, W. M.; Hyun, M. H. *Ibid.* **1984**, *49*, 3043. (g) Pirkle, W. H.; Hyun, M. H.; Bank, B. *J. Chromatogr.* **1984**, *316*, 585. (h) Pirkle, W. H.; Hyun, M. H.; Tsipouras, A.; Hamper, B. C.; Banks, B. *J. Pharm. Biomed. Anal.* **1984**, *2*, 173. (i) See: Pirkle, W. H.; Pochapsky, T. C. *J. Am. Chem. Soc.* **1987**, *109*, 5975–5982 for related references.
(22) Aldrich Fine Chemicals Catalog, 1986, p 1306 and references therein.
(23) Bakerbond Chiral Phase Analytical HPLC Column, DNBPG (Covalent), Product No. 7113-0, J. T. Baker Research Products.
(24) Andersen, L.; Berg, U.; Petterssen, I. *J. Org. Chem.* **1985**, *50(4)*, 493.
(25) Challis, B. C.; Challis, J. A. In *Comprehensive Organic Chemistry*; Sutherland, I. O., Ed.; Pregamon Press: Oxford, 1979; Chapter 9.9.

Table II. Fully Relaxed MM2D Geometries of *S*-Analyte **1**

name	torsion angeles (degs) α C_{25}–C_6–C_{15}–C_{27}	torsion angeles (degs) β C_6–C_{15}–O_{16}–H_{30}	rel energy (kcal mol^{-1})
A1	84.7	−137.8	0.00
A2	83.5	−28.3	0.14
A3	84.2	107.0	2.74

as well as by MNDO semiempirical molecular orbital methods. The two unique degrees of freedom that characterize the templating ability of **3** and related phases are torsion angles, ω and δ, defined by atoms C_7–N_9–C_{11}–H_{15} and N_9–C_{11}–C_{23}–O_{24}, respectively. With standard dihedral driver methods,[28] all of the conformational space was searched for CSP analogue **3**. The results are summarized in Table I.

We find **3** and related phases to possess multiple minima on their multidimensional potential energy surfaces. Several of these minima are significantly populated at ambient temperatures. A generalization is that the potential energy surfaces of **2** and related CSP's have flat topological features with broad, shallow regions around the minima. Additionally, the energy barriers separating minima on these surfaces are usually between 2 and 5 kcal mol^{-1}, ensuring rapid interconversion between conformational states. Because of this inherent flexibility we have adopted the policy of using more than one conformation of the CSP in the analysis of diastereomeric complexes.

For *R*-CSP analogue **3**, the global minimum with $\omega = -60°$, $\delta = -132°$ accounts for 91% of the conformer population while the conformation with $\omega = -165°$, $\delta = 140°$ accounts for 8% of the population. Hence these two forms alone account for approximately 99% of the conformational states of the CSP. These results have been analyzed by us in detail,[26] are consistent with conformations invoked in chiral recognition by Pirkle,[21] and will not be further discussed here.

The analyte **1** was studied in a similar manner. The two important torsional degrees of freedom are α and β defined by C_{25}–C_6–C_{15}–C_{27} and C_6–C_{15}–O_{16}–H_{30}, respectively. Our results are summarized in Table II. The two conformations with $\alpha = 84°$, $\beta = -138°$ and $\alpha = 84°$, $\beta = -28°$ account for >99% of the analyte conformations populated at 298 K. Both of these conformations have the acidic methine hydrogen nearly in the plane of the anthryl ring while the OH and CF_3 groups are bisected by the anthracene. The difference between the two conformations involves the orientation of the hydroxyl hydrogen. The global minimum has the hydrogen directed toward a fluorine of the CF_3 group (an intramolecular hydrogen bond) while the other conformer has the hydrogen directed away from the CF_3 group. These results are consistent with the observation of intramolecular hydrogen bonding found in 1-fluoroethanol.[29]

B. Diastereomeric Complexes. Together CSP1 and CSP2 account for over 98% of the chiral phase conformations. Likewise A1 and A2 account for 99% of the analyte conformations. Hence, by considering four combinations of rigid CSP with rigid analyte (CSP1·A1, CSP1·A2, CSP2·A1, CSP2·A2) we account for >98% of the probability of finding the CSP and the analyte in their minimum energy conformations.

To calculate the free energy $\bar{E}$ we must locate all unique minimum energy diastereomeric complexes.[30] Hence we were concerned about the step size for incremental movement of analyte around the CSP. Furthermore, for each increment in latitude θ and longitude ϕ, we were concerned about the number of analyte orientations to sample. We started by varying θ and ϕ in 20° increments. At each (θ,ϕ) point the analyte was assigned 48 axes with 18 unique orientations per axis and minimum energy structures were located. The process was repeated with 10° increments of θ and ϕ, 99 axes on the analyte, and 36 orientations per axis. With this "higher resolution" search new minima were detected. This was repeated with higher resolution sampling until no new minimum energy structures could be located. The optimum sampling strategy involved moving the analyte around the CSP in 10° increments and assigning 48 unique axes to the analyte with 18 orientations per axis. This resulted in 155 040 unique samples for each of the eight complexes considered (four for *R*·*R* and four for *R*·*S*).

By employing this sampling regimen and using a dielectric constant of 1.00, the intermolecular potential energy was calculated for the C^R·A^R and C^R·A^S complexes of CSP analogue **3** with analyte **1**. The energy of the most stable analyte orientation for each latitude, θ, and longitude, ϕ, was then used to generate contour maps as described in an earlier communication.[31] These plots represent the lowest intermolecular energy as the analyte rolls over the van der Waals surface of the CSP and are informative because they provide insight about regions around the CSP where the analyte is most likely to bind. Additionally they indicate the barriers separating the binding sites on the CSP. The intermolecular potential energy surfaces for these diastereomeric complexes are strikingly similar and suggest that binding of the two analytes occur at the same region(s) around the CSP but perhaps in different ways (vide infra). For analyte **1** we find two especially stable binding sites corresponding to "front-side" and "back-side" docking. These low-energy binding regions are separated by ~6 kcal mol^{-1} energy barriers. Other less stable binding sites are also found.

The final results of our computations of $\bar{E}$ using the sampling procedure described above and eq 13 are presented in Table III.

V. Discussion

In Table III, "complex designation" indicates the conformations of CSP being paired with those of analyte. The two conformers of CSP listed (CSP1 and CSP2) and the two of analyte (A1 and A2) account for over 98% of all conformational states populated by those molecules under chromatographic conditions. TS is the 298 K entropic term, H is the enthalpic term, and $\bar{E}$ is the difference of these. The quantity % $\bar{E}$ is the percent of the total energy $\bar{E}$ due to each conformational pair. The "most retained" enantiomer is the one for which the value of $\bar{E}$ is most negative.

The results in Table III are illuminating. Most important is the prediction of which optical isomer is most retained on the column. Interestingly, the calculation of binding energies appears to be conformation dependent. The complex designated CSP1·A1 and the one designated CSP2·A1 indicate the *R* enantiomer to be most retained while the complexes designated CSP1·A2 and CSP2·A2 indicate the *S* enantiomer to be more retained. The total interaction energies summed over all orientations of all complexes predicts the *S* enantiomer will be more retained on the column. This is in agreement with experiment. The meaning of small (~0.1 kcal mol^{-1}) energy differences in these calculations should be addressed. Certainly the accuracy of molecular mechanics is not within this range. However, because we are comparing virtually identical systems, the molecular mechanics errors in one complex will be the same as those in the other complex. The near cancellation of errors provides us with small but meaningful energy differences between the complexes.

In a preliminary communication[31] we reported on the binding of analyte **1** with CSP analogue **3**. In that note we considered the single most stable conformations of the CSP and of the analyte only (this corresponds to CSP1·A1). The most stable, rigid-body intermolecular complex for the *RR* and the *RS* diastereomers were

(26) (a) Lipkowitz, K. B.; Landwer, J. M.; Darden, T. *Anal. Chem.* **1986**, *58*, 1611. (b) Lipkowitz, K. B.; Malik, D. J.; Darden, T. *Tetrahedron Lett.* **1986**, *27(16)*, 1759. (c) Lipkowitz, K. B.; Demeter, D. A.; Parish, C. A.; Landwer, J. M.; Darden, T. *J. Comput. Chem.* **1987**, *8(6)*, 753. (d) Lipkowitz, K. B.; Demeter, D. A.; Landwer, J.; Parish, C. A.; Darden, T. *Ibid.*, accepted for publication 1987.

(27) Unpublished results: L. B. Rogers and M. Still, Department of Chemistry, University of Georgia.

(28) Wiberg, K. B.; Boyd, R. H. *J. Am. Chem. Soc.* **1972**, *94*, 8426.

(29) Hoffmann, W. F., III; Shirk, J. S. *Chem. Phys.* **1983**, *78*, 331 and references therein.

(30) The location of origin is arbitrary; we chose to place the origins on the stereogenic centers of the CSP and analyte. The calculations should be, and are, independent of origin. The intermolecular potential energy maps are simply phase-shifted when the origins are moved to new locations.

(31) Lipkowitz, K. B.; Demeter, D. A.; Parish, C. A.; Darden, T. *Anal. Chem.* **1987**, *59*, 1731.

Table III. Results from the Calculation of $\bar{E}$ for CSP **3** with Trifluoroanthrylethanol **1**

complex designation	$C^R \cdot A^R$				$C^R \cdot A^S$				most retained
	% $\bar{E}$	$\bar{E}$	H	TS	% $\bar{E}$	$\bar{E}$	H	TS	
CSP1·A1	55.4	−4.22	−4.18	0.04	54.4	−4.17	−4.12	0.05	*R*
CSP1·A2	36.9	−2.81	−2.80	0.01	38.0	−2.91	−2.90	0.01	*S*
CSP2·A1	4.4	−0.34	−0.33	0.00	4.2	−0.32	−0.32	0.00	*R*
CSP2·A2	3.4	−0.26	−0.25	0.0	3.5	−0.27	−0.26	0.00	*S*
Total	100.0	−7.62	−7.57	0.05	100.0	−7.67	−7.61	0.06	*S*

located. The global minimum from that search favors binding of the *S* enantiomer by ca. 0.35 kcal mol^{-1}. In contrast the complex designated CSP1·A1 in Table III suggests the *R* rather than *S* enantiomer to have a larger binding energy. We find here that by considering higher energy intermolecular complexes in addition to the global minimum the prediction of the most retained enantiomer is reversed. How the higher energy orientations (weighted in a Boltzman way) offset the prediction based upon the global minimum alone is not yet clear. Nonetheless these results imply that single, minimum energy structures alone, even global minima, inadequately describe binding and that all intermolecular energies must be considered.

Another aspect of our results already mentioned above but highlighted here is that *the prediction of enantioselectivity is conformation dependent*. The two instances where *R* is most retained involve the binding of analyte in its most stable form to the CSP (in either form). The reason for this is that A1 has an intramolecular hydrogen bond that cannot be used for hydrogen bonding to the CSP as can A2.

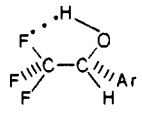

A1

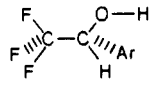

A2

Choosing minimum energy states for both isolated CSP and isolated analyte could be an unrealistic approach for describing the shapes of these molecules in the presence of each other. The rigid body approach in our analysis of analyte binding is tantamount to Fischer's lock-and-key model.[32] One would expect, however, that as analyte binds with CSP, both the CSP and the analyte will change shape in the real system to accommodate a better fit with the other partner. To determine how much "induced-fit" distortion of CSP occurs, we performed some calculations fully relaxing the 50 lowest energy intermolecular complexes and then comparing the geometry of the CSP before and after optimization. Upon full inter- and intramolecular relaxation, the molecules further entwine with a concomitant drop in energy. There were no gross structural reorganizations observed for any of the complexes. Indeed the largest conformational difference between CSP before and after optimization had a root-mean-square deviation of 0.155 Å for all 40 atoms compared. The smallest difference was root-mean-square deviation of 0.015 Å. The *average* root-mean-square deviation of all atoms on CSP analogue **3** before and after intermolecular relaxation is only 0.074 Å. Hence our rigid body approach to computing structural features of the diastereomeric complexes accurately reproduces those structural features derived from a far more expensive full optimization.

The way the analyte selectively binds to the CSP is fairly complex. Difference plots between intermolecular potential energy surfaces for *RR* and *RS* diastereomeric complexes are helpful for locating regions around the CSP responsible for enantioselection, but a visualization of how the CSP embraces the analyte is needed. To describe this, we generated stereographic plots of a large number of the minimum energy diastereomeric complexes. Our intention was to find binding motifs that describe how *R* and *S* analyte associate with the CSP. A representative number of these plots are presented in Figure 2. These are "snapshots" of the minimum energy orientation of analyte as it rolls over the van der Waals surface of the CSP. Most, but not all, complexes have a π–π interaction between the anthryl ring of the analyte with the 3,5-dinitrobenzoyl moiety of the CSP. In addition to this we find a variety of intermolecular hydrogen bonding combinations for both the *RR* and *RS* complexes.

A chiral recognition model for binding of **1** to **2** has been previously suggested by Pirkle. In that model the analyte binds to the CSP via (i) π acid–π base attractions, (ii) hydrogen bond donation from **1** to the 3,5-dinitrobenzoyl's carbonyl oxygen, and (iii) an association of the acidic carbinyl hydrogen on **1** with a suitable binding site on **2** (probably the other carbonyl oxygen). This interpretation is based upon the 3-point attachment theory of Dalgleish[33] and, albeit an oversimplication, describes the major interactions responsible for binding. Molecular mechanics, based upon pairwise additive interactions of all atoms on CSP with all atoms on **1**, makes it difficult to describe intermolecular interactions this way. Nonetheless we do find a binding motif for *S* analyte that differs from that of *R* analyte. These differences were pointed out by us in an earlier communication[31] and may be summarized as follows. For the *R* enantiomer the hydroxyl serves as a hydrogen bond donor coordinating with the amide carbonyl oxygen on the CSP. For the *S* enantiomer, in contrast, the analyte is rotated 180° and the analyte serves as a hydrogen bond acceptor. In this orientation the N–H of the CSP amide is directed toward the lone pair of electrons on the oxygen of the analyte's hydroxyl group. In both instances the phenyl group on the CSP serves only as a steric barrier to keep analytes from strongly binding to the rearside.

In the present work we had the opportunity to relax all intra- and intermolecular degrees of freedom. Upon full relaxation of the rigid body minimum energy diastereomeric complexes cited in our earlier communication, the analyte slides over the π surface of the CSP and the OH group rotates to better form a hydrogen bond to the amide carbonyl oxygen. Even with this movement we note the hydroxyl hydrogen is not in the best position to form a hydrogen bond to the dinitrobenzoyl moiety. Murray-Rust and Glusker[34] assessed hydrogen bonding to carbonyls and found that hydrogen donation is preferred in the plane of the C=O. The formation of charge transfer complexes in this analyte–CSP association holds the analyte perpendicular to the plane of the amide group and consequently introduces a non-optimal arrangement for intermolecular hydrogen bonding. The results of these full geometry optimizations do not change the major conclusions of our earlier work.

Both ours and Pirkle's chiral recognition models have similar intermolecular interactions responsible for the observed enantioselectivity. Given the nature of these interactions, it will be difficult to design experiments to distinguish between the two models. More problematic, through, may be the fact that multiple mechanisms are responsible for the separation. Indeed, more than one chiral recognition model has already been proposed by the Pirkle group to account for reversals in enantioselection as analyte chain lengths are increased.[35]

VI. Conclusions

Placing a racemic mixture on a chromatographic column composed of a suitable chiral support should, in principle, allow

(32) Fischer, E. *Ber. Dtsch. Chem. Ges.* **1894**, *27*, 2985.

(33) Dalgleish, C. *J. Chem. Soc.* **1952**, *137*, 3940.
(34) Murray-Rust, P.; Glusker, J. P. *J. Am. Chem. Soc.* **1984**, *106*, 1018.
(35) Pirkle, W. H.; Hyun, M. H.; Banks, B. *J. Chromatogr.* **1984**, *316*, 585.

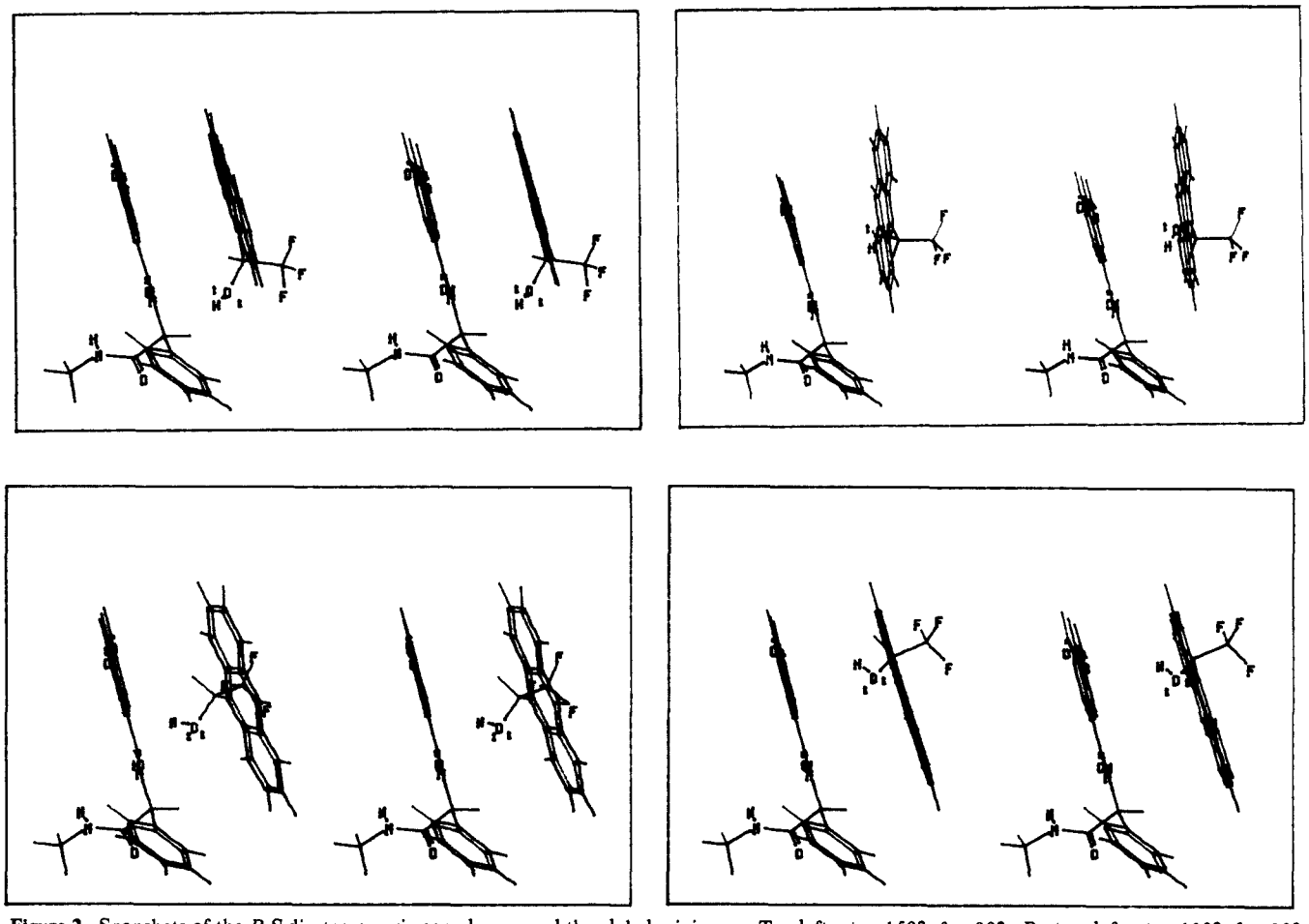

Figure 2. Snapshots of the *R*·*S* diastereomeric complex around the global minimum. Top left: $\phi = 150°, \theta = 80°$. Bottom left: $\phi = 130°, \theta = 80°$. Top right: $\phi = 90°, \theta = 50°$. Bottom right: $\phi = 120°, \theta = 80°$.

the enantiomers to migrate through the column at different rates and be collected individually. Although this technique has long been recognized as feasible and some chiral chromatographic columns have been developed, it is only recently that they have been marketed and incorporated into the bench chemist's ritual.

Precisely how these chromatographic columns work is not known; clearly short-lived diastereomeric complexes between optical analytes and chiral phase are formed. The relative retention of optical analytes depends, in part, upon these diastereomeric interactions. Of concern to us was the possibility that the CSP could exist in more than one conformation. It was felt that higher energy and subsequently less populated shapes of the CSP may very effectively discriminate between enantiomers while more stable, highly populated conformers may ineffectively discriminate between enantiomers. Pirkle had already recognized this problem by stating "...the conformational behavior of both solute and stationary phase must be considered in advancing chiral recognition models to account for observed chromatographic behavior."[36] E, the column averaged free energy of interaction, accounts for this by including in a statistically weighted manner (i) conformational states of the CSP, (ii) conformational states of analyte, and (iii) all possible orientations of analyte with respect to the CSP. Indeed the prediction of which enantiomer of 2,2,2-trifluoro-1-(9-anthyl)ethanol is most retained on a commercially available CSP was found to be conformation-dependent. In this example the conformational dependence was attributed to the analyte, not the CSP.

Contour maps of the intermolecular potential energies were especially useful for interpretation of enantiomer binding. For chiral stationary phase **1** we find two important regions for analyte binding. One region corresponds to front-side association while the other corresponds to rearside association. These binding sites are separated by ~6 kcal mol^{-1} energy barriers.

Finally, by inspecting all possible modes of analyte binding to CSP analogue **3**, we developed a new chiral recognition model. This model has features similar to the one proposed by Pirkle, but it is different and merits further testing. Understanding from first principles how stereodifferentiation takes place is important. Although our focus has been on chiral chromatography, extensions to drug design or other areas of science where molecular recognition is important are possible.

Acknowledgment. This work was funded by the donors of the Petroleum Research Fund, administered by the American Chemical Society.

(36) Pirkle, W. H.; Finn, J. M.; Hamper, B. C.; Schreiner, J.; Pribish, J. R. In *Asymmetric Reactions and Processes in Chemistry*; Eliel, E., Otsuka, S., Eds.; ACS Symp. Ser. 185; American Chemical Society: Washington, DC, 1982; p 256.